



# Photogeneration of hydrogen from water using CdSe nanocrystals demonstrating the importance of surface exchange

Amit Das, Zhiji Han, Mohsen Golbon Haghighi, and Richard Eisenberg<sup>1</sup>

Department of Chemistry, University of Rochester, Rochester, NY 14627

This contribution is part of the special series of Inaugural Articles by members of the National Academy of Sciences elected in 2010.

Contributed by Richard Eisenberg, September 4, 2013 (sent for review July 16, 2013)

**Unique tripodal S-donor capping agents with an attached carboxylate are found to bind tightly to the surface of CdSe nanocrystals (NCs), making the latter water soluble. Unlike that in similarly solubilized CdSe NCs with one-sulfur or two-sulfur capping agents, dissociation from the NC surface is greatly reduced. The impact of this behavior is seen in the photochemical generation of H<sub>2</sub> in which the CdSe NCs function as the light absorber with metal complexes in aqueous solution as the H<sub>2</sub>-forming catalyst and ascorbic acid as the electron donor source. This precious-metal-free system for H<sub>2</sub> generation from water using [Co(bdt)<sub>2</sub>]<sup>−</sup> (bdt, benzene-1,2-dithiolate) as the catalyst exhibits excellent activity with a quantum yield for H<sub>2</sub> formation of 24% at 520 nm light and durability with >300,000 turnovers relative to catalyst in 60 h.**

photochemistry | solar energy | catalysis | water splitting | quantum dots

Artificial photosynthesis (AP) represents an important strategy for energy conversion from sunlight to storage in chemical bonds (1–4). Unlike natural photosynthesis in which CO<sub>2</sub> + H<sub>2</sub>O are converted into carbohydrates and O<sub>2</sub>, the key energy-storing reaction in AP is the splitting of water into its constituent elements of hydrogen and oxygen (5–16). As a redox reaction, water splitting can be divided into two half-reactions, of which the light-driven generation of H<sub>2</sub> is the reductive component. Many systems for the photogeneration of H<sub>2</sub> have been described over the years and they typically consist of a light absorber, a catalyst for H<sub>2</sub> formation, and sources of protons and electrons. For systems that function in aqueous media, the protons are provided by water, whereas for nonaqueous systems, the protons are provided by weak, generally organic acids. The source of electrons in these photochemical systems is generally a sacrificial electron donor—that is, a compound that decomposes following one electron oxidation.

Reports of the light-driven generation of hydrogen date back more than 30 y, beginning with a multicomponent system containing [Ru(bpy)<sub>3</sub>]<sup>2+</sup> (where bpy is 2,2'-bipyridine) as the chromophore or photosensitizer (PS) and colloidal Pt as the catalyst for making H<sub>2</sub> from protons and electrons (17). In these and many subsequent systems, electron mediators were used to accept an electron from the excited chromophore, PS\*—thereby serving as an oxidative quencher—and transfer it to the catalyst. Whereas two of the initial mediators were bpy complexes of rhodium and cobalt (17, 18), the overwhelming majority of electron mediators in these systems were dialkylated 2,2'- and 4,4'-bipyridines and their derivatives (19–22). The most extensively used of these mediators was methyl viologen (MV<sup>2+</sup>, dimethyl-4,4'-bipyridinium, usually as its chloride salt). These mediators were subsequently found to undergo deactivation in their role by hydrogenation (23, 24). The sacrificial electron donors used in these studies depended on system pH and were generally based on compounds having tertiary amine functionality for decomposition following oxidation, such as triethylamine (TEA), triethanolamine (TEOA), and ethylenediamine-*N,N,N',N'*-tetraacetic acid (EDTA) (17, 19–22). A different electron

mediator during the early studies on light-driven generation of hydrogen was found to be TiO<sub>2</sub>, which when platinized served as both the mediator and the catalyst (25–28).

During the more than three decades that have passed since the initial reports (17, 19–22, 25–27), every aspect and component of photochemical proton reduction systems have been investigated with the goal of increasing activity and durability. These include new molecular catalysts and different photosensitizers ranging from other metal complexes with long-lived charge-transfer excited states to strongly absorbing organic dyes. With a view toward the possible long-term utilization of hydrogen from solar-driven water splitting, efforts have expanded over the past decade to use components that contain only earth-abundant elements and thus to remove Pt, Pd, Ru, Ir, and Rh from such systems. In this regard, photochemical proton reduction systems have been reported in which complexes of cobalt, nickel, and iron are found to function as catalysts for hydrogen generation (18, 29–41). A number of these complexes were inspired by the active sites of hydrogenase enzymes in which Fe is, and Ni may be, present, and a pendant organic base is thought to help as a proton shuttle to a postulated metal-hydride intermediate for H<sub>2</sub> formation (30, 31, 35, 37, 42, 43).

Another set of complexes investigated as catalysts for proton reduction are complexes of Co having diglyoxime-type ligands that form a pseudomacrocyclic structure (that is, two diglyoxime ligands linked together by either H bonds or BF<sub>2</sub> bridges) (44–54). Although many of these studies with regard to catalyst development were, and are, based on electrocatalytic generation of H<sub>2</sub> (44–50), more recent efforts have used the cobaloxime catalysts

## Significance

Conversion of solar energy into chemically stored energy via artificial photosynthesis (AP) represents a key strategy in renewable energy. Systems for AP that split water reduce aqueous protons to H<sub>2</sub> fuel and oxidize water to make O<sub>2</sub>. The present study on the light-driven generation of H<sub>2</sub> describes a new, highly active, and durable system with components made solely of earth-abundant elements. The light absorber in this system consists of quantum-confined CdSe nanocrystals that are made water soluble through surface binding agents. Realization of the effects of surface ligand exchange on system activity stimulated the new compounds reported here that bind more strongly to the nanocrystals through tridentate coordination and allow assessment of catalyst activity for H<sub>2</sub> generation.

Author contributions: A.D., Z.H., and R.E. designed research; A.D., Z.H., and M.G.H. performed research; A.D., Z.H., M.G.H., and R.E. analyzed data; and A.D., Z.H., and R.E. wrote the paper.

The authors declare no conflict of interest.

<sup>1</sup>To whom correspondence should be addressed. E-mail: Eisenberg@chem.rochester.edu.

This article contains supporting information online at [www.pnas.org/lookup/suppl/doi:10.1073/pnas.1316755110/-DCSupplemental](http://www.pnas.org/lookup/suppl/doi:10.1073/pnas.1316755110/-DCSupplemental).

in light-driven systems (51–54). Photosensitizers in these investigations have been either charge transfer metal complexes of Ru(II), Ir(III), Re(I), and Pt(II) or organic dyes. Although some of these systems exhibited significant activity for making H<sub>2</sub>, all of them suffered from instability that led to cessation of activity after periods ranging from 6 h to 30 h.

The use of the cobaloxime catalyst CoCl(pyr)(dmg)<sub>2</sub> (where dmg is dimethylglyoximate anion) in conjunction with organic dyes as PS provided the first molecular systems for visible light-driven proton reduction to H<sub>2</sub> that were free of precious metals (55–57). The most effective of these used a Se-derivatized rhodamine dye as the chromophore with TEOA as the sacrificial electron donor, yielding good activity with an initial turnover frequency (TOF) > 5,000/h (vs. PS) and total turnover number (TON) of 9,000 after 8 h (57). Analysis of this system revealed that it functioned via reductive quenching of PS\* by TEOA and subsequent electron transfer from PS<sup>-</sup> to the catalyst. Another organic dye-catalyst system that also exhibited good activity used fluorescein (Fl) as PS and a nickel pyridinethiolate (pyS) catalyst in pH 11 media with TEA as the sacrificial donor. This system also was found to function via reductive quenching of PS\* by the electron donor, rather than by direct electron transfer from PS\* to the catalyst or an electron mediator (37). A significant number of reviews provide detailed accounts of the various systems studied and their effectiveness with regard to H<sub>2</sub> generation (1, 58–64). However, all of them, which contain molecular light absorbers [charge transfer (CT) metal complexes and organic dyes], suffer from photoinstability during prolonged irradiation. Additionally, the molecular catalysts for H<sub>2</sub> generation may undergo deactivation, as has been established for the Co glyoximate complexes.

In an analysis for genuinely viable systems for proton reduction and water oxidation in solar-driven water splitting, Bard and Fox addressed the question of component stability and indicated a need to focus on the use of semiconductors (SCs) as light absorbers based on the wide energy range of SC bandgaps, the electron transfer properties of excited semiconductors, and their potential stability under prolonged irradiation (65). Although the use of semiconductors for photochemical water splitting dates back to a report by Fujishima and Honda in 1972 with TiO<sub>2</sub> and UV light, the challenge was to use SCs with absorption maxima that better matched the solar spectrum (66). There have been numerous reports describing efforts in this direction and several recent reviews offer a summary of systems used and results obtained (67–75). Semiconductor nanoparticles that exhibit size-constrained electronic properties represent a large and important class of possible light absorbers for the two half-reactions of water splitting. These nanoparticles, which are referred to as quantum dots (QDs) and nanocrystals (NCs), represent a fertile area of study in the context of energy conversion

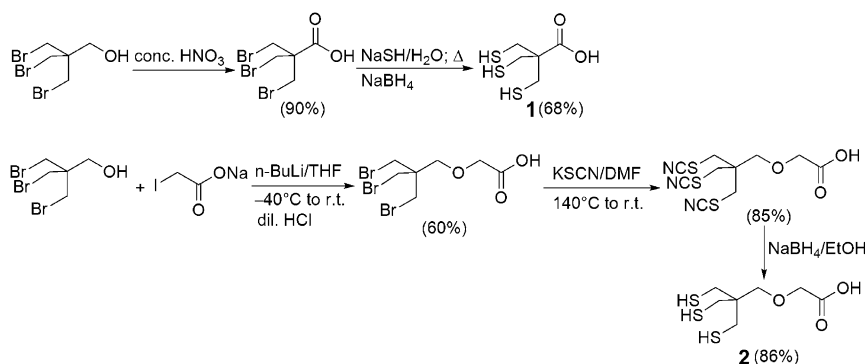
because their bandgaps can be adjusted via their preparation and their solubility can be controlled by their surface stabilizers or capping agents (76). In this way, NCs can offer unique size-dependent optical properties and stronger light absorption over a wider spectral range than do molecular PSs (68, 76). In fact, NCs as light absorbers in combination with precious metal proton reduction catalysts or with Fe-Fe hydrogenase have been studied, yielding interesting photocatalytic systems (77–81).

We recently communicated such a system for carrying out H<sub>2</sub> formation from aqueous protons that possessed great durability and impressive activity. The light absorber in this system was water-solubilized CdSe NCs, the catalyst was an *in situ*-formed complex of Ni<sup>2+</sup> with the water-solubilizing agent dihydroliipoic acid (DHLA), the electron source was ascorbic acid (AA), and the system medium was water at pH 4.5. TONs of more than 600,000 were reported for one set of conditions, using 520 nm light, whereas for a different set of conditions durability over 15 d was found (82). Water solubilization of CdSe NCs using agents such as 3-thiopropionic acid and DHLA has been known for some time, with DHLA more strongly binding via chelation (83–85). In the system that we previously reported for H<sub>2</sub> production, however, dissociation of DHLA from the CdSe NCs was an essential aspect of its operation to form the Ni-DHLA catalyst (82). On the other hand, the dissociation of DHLA from the CdSe NCs was also found to negatively affect the examination of preformed catalysts because of competing exchange reactions involving DHLA and the catalyst ligands.

In our current study, we report a unique hydrogen-generating system using CdSe NCs with much less labile water-solubilizing capping agents. This unique system, which is more durable, allows assessment of the activity of successful H<sub>2</sub>-generating catalysts that had been established electrochemically or in a different photochemical system. The reduced lability of the water-solubilizing agent is based on having three S donors in close proximity to each other for the formation of a more stable bridging structure to the CdSe nanoparticle.

## Results and Discussion

The capping agents and their syntheses are shown in Scheme 1. For **1**, pentaerythritoltribromide is first oxidized to the corresponding pivalic acid derivative, after which the Br substituents are replaced by the corresponding SH groups (see *Materials and Methods* for details). For **2**, pentaerythritoltribromide is first reacted with sodium iodoacetate to form an ether linkage between the tribromo and acetic acid fragments. The Br substituents are replaced in the following steps with SCN and then reduced to SH, resulting in the formation of ligand **2** (see *Materials and Methods* for details). The NMR data for both **1** and **2** fit well for the proposed molecular structures and elemental analytical data match with the calculated values (*SI Appendix, Figs. S3 and S6 and Materials and Methods*). Electrospray ionization mass spectrometry



**Scheme 1.** Synthesis of tridentate capping agents **1** and **2** with yields for individual steps.

(negative mode) of **1** and **2** shows molecular ion signals at 197.18 and 241.18, corresponding to  $(1-H)^-$  and  $(2-H)^-$ , respectively. Crystallographic structural determinations of **1** and **2** also confirm the identities and structures of the two capping agents (*SI Appendix*).

It should be noted that a similar water-solubilizing capping agent with the same arrangement of S donors has been reported previously in the use of chalcogen-based nanoparticles for in vivo imaging. In that particular study, water solubilization was made possible by a long polyethylene glycol (PEG) chain attached to the pentaerythritol O-atom (86). However, because of the need for electron transfer between the CdSe NCs and the catalyst in the present study, we chose to use the short linkages to hydrophilic carboxylates in **1** and **2** for water solubilization. The same arrangement of the  $(HSCH_2)_3C^-$  moiety has also been used to make branched organometallic structures in which the S-donor atoms bridge adjacent metal atoms (Rh, Ir) as envisioned for the CdSe NCs binding (87).

Aqueous solubilization of the CdSe NCs using **1** and **2** was conducted according to previously reported procedures (82). First, trioctylphosphine oxide (TOPO)-capped CdSe NCs were synthesized following a literature procedure (82, 88) and characterized by UV-vis spectroscopy (*Materials and Methods*). The size of the NCs thus generated was in the range of 2.5–2.7 nm with an energy difference between the valence band (VB) and the conduction band (CB) edges of  $\sim 2.4$  eV. Exchange of the TOPO ligand for **1** or **2** is done in MeOH followed by precipitation upon the addition of ethyl acetate, centrifugation, and redissolution in water. The exchange process does not affect the size of the NCs, as determined from UV-vis spectra of the NCs before and after exchange (Fig. 1). The hydrophilic carboxylate groups of **1** and **2** make the NCs to which they are bound soluble in slightly basic aqueous solution. Care must be taken during purification of **1**- and **2**-bound CdSe NCs that all free hydrophilic capping agents in solution have been removed. The absence of dissociation of **1** or **2** from the surface is supported by a  $^1H$  NMR experiment in which resonances of the capping agent are not detected in solution after 24 h (*Materials and Methods*), in contrast to the direct observation of DHLA resonances when the experiment is carried out with DHLA-CdSe NCs. Once purified, **1**- and **2**-CdSe NCs are stable under atmospheric conditions and can be stored for long periods in a freezer without direct irradiation of light.

Following successful synthesis of the  $S_3$ -capped NCs, their activity in the photochemical reduction of aqueous protons to  $H_2$  was examined. The initial conditions used were similar to those

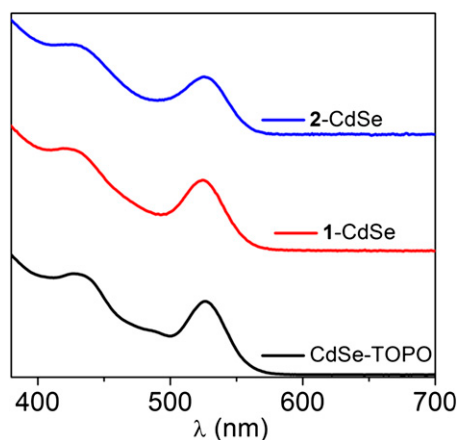


**Fig. 1.** UV-vis spectra of CdSe-TOPO NCs in hexane (black), 1-CdSe NCs (red), and 2-CdSe NCs (blue) in water (1-CdSe and 2-CdSe were prepared from the same batch of CdSe-TOPO NCs).

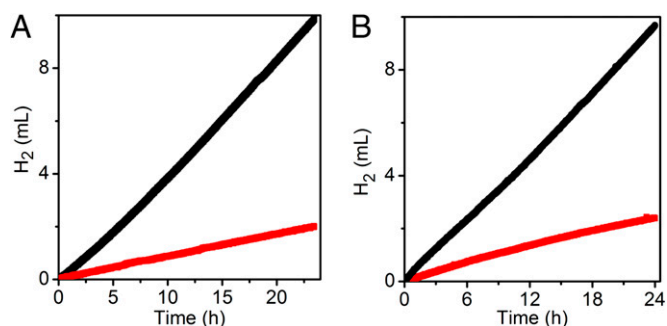
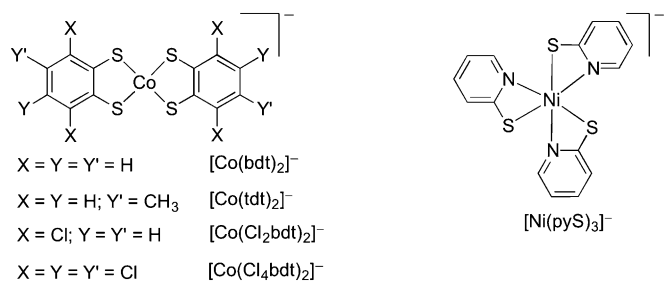


**Fig. 2.** (A and B) Photocatalytic hydrogen production from a system containing (A) 1-CdSe NCs (525 nm) (6.0  $\mu$ M), AA (0.3 M), 1.0  $\mu$ M  $[Ni(NO_3)_2]$  (red), and 1.0  $\mu$ M  $[Ni(NO_3)_2]$  + 2 eq of DHLA (black) and (B) 2-CdSe NCs (525 nm) (6.0  $\mu$ M), AA (0.3 M), 1.0  $\mu$ M  $[Ni(NO_3)_2]$  (red), and 1.0  $\mu$ M  $[Ni(NO_3)_2]$  + 2 eq of DHLA (black) in 5 mL water at pH 4.5 upon irradiation with 520 nm LED at 15  $^\circ$ C and 1 atm initial pressure of  $N_2:CH_4$  (79:21 mol %) with  $CH_4$  as an internal standard for  $H_2$  quantification by GC analysis.

in the earlier report of the system composed of DHLA-CdSe NCs and aqueous soluble  $Ni(NO_3)_2$  as the catalyst precursor for  $H_2$  generation. The specific conditions were 1  $\mu$ M of  $Ni(NO_3)_2$ , 6  $\mu$ M of **1**- or **2**-capped CdSe NCs (525 nm), and 0.3 M AA at pH 4.5 with irradiation from green light-emitting diodes (LEDs) ( $\lambda = 520$  nm, 13 mW/cm $^2$ ) at 15  $^\circ$ C. Yields of  $H_2$  from this system were relatively small (Fig. 2) because of the much reduced dissociation of **1** or **2** from the NC surface, thereby eliminating the possibility of in situ generation of an active Ni catalyst for hydrogen formation. This view was confirmed when DHLA (2 equivalents) was added to the systems, resulting in very substantial increases in  $H_2$  produced as a consequence of the formation of the Ni-DHLA catalyst that had been postulated to form (Fig. 2). This result clearly indicates the importance of DHLA dissociation and exchange in the previously reported system and the relative inertness of **1** and **2** from the NC surface in the present system (82). The addition of 2 equivalents of **1** to the 1-CdSe/ $Ni(NO_3)_2$ /AA system also resulted in an increase in activity of  $H_2$  generation (*SI Appendix*), which clearly supports the view that there is no dissociation of **1** from the NC surface to bind with  $Ni^{2+}$ .

The inertness of **1** and **2** from the CdSe NCs allows an examination of previously reported molecular catalysts in a CdSe NC-photosensitized system without interference of free capping agent in solution and consequent ligand/capping agent exchange reactions that can occur on the catalyst as was found when DHLA was used. This is seen dramatically for the Co bis dithiolene complex  $[Co(bdt)_2]^-$  (Scheme 2), which is an excellent catalyst for photochemical hydrogen generation when used with  $[Ru(bpy)_3]^{2+}$  as the photosensitizer and AA as the sacrificial electron-donating agent. Despite its activity, this specific system was not long-lived ( $< 6$  h) as a result of photosensitizer and



**Scheme 2.** Structures of Co bis dithiolene and Ni pyridylthiolate complexes examined as catalysts.



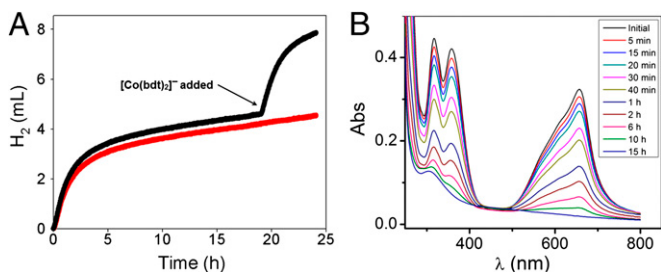


**Fig. 3.** (A) Photocatalytic hydrogen production from a system containing DHLA CdSe NCs (540 nm) (6.0  $\mu\text{M}$ ),  $[\text{Co}(\text{bdt})_2]^-$  (1.0  $\mu\text{M}$ ), and AA (0.5 M) in  $\text{H}_2\text{O}$  (5.0 mL) at pH 4.5 upon irradiation with 520 nm LED at 15 °C and 1 atm initial pressure of  $\text{N}_2:\text{CH}_4$  (79:21 mol %) with  $\text{CH}_4$  as an internal standard for  $\text{H}_2$  quantification by GC analysis. (B) UV-vis spectral changes of a solution containing 20  $\mu\text{M}$   $[\text{Co}(\text{bdt})_2]^-$  and 0.3 mM DHLA over a period of 15 h.

catalyst decomposition (38, 39). The deleterious effect of ligand/capping agent exchange was observed when the  $[\text{Co}(\text{bdt})_2]^-$  catalyst was used with the DHLA-CdSe NCs as the photosensitizer. Although the initial activity of the system was high, it diminished rapidly. Because the loss of activity could not be due to decomposition of the DHLA-CdSe photosensitizer, the decline in performance appeared to be due to the  $[\text{Co}(\text{bdt})_2]^-$  catalyst. This was confirmed by the addition of  $[\text{Co}(\text{bdt})_2]^-$  to the system following the loss of activity in  $\text{H}_2$  generation, leading to restoration of activity as shown in Fig. 3A. The amount of  $[\text{Co}(\text{bdt})_2]^-$  added after 18 h was the same as that initially used and the restored  $\text{H}_2$ -generating activity matched well with the initial rate.

The basis of the reduction in  $\text{H}_2$ -generating activity for the DHLA-CdSe NC/ $[\text{Co}(\text{bdt})_2]^-$ /AA system had to result from the destruction of the  $[\text{Co}(\text{bdt})_2]^-$  catalyst as a consequence of the free DHLA in solution. This was shown in two sets of experiments. In the first, the UV-vis spectra of  $[\text{Co}(\text{bdt})_2]^-$  and 15 eq of DHLA [similar to the amount of DHLA that dissociates from the CdSe NCs (82)] in water were monitored over time as shown in Fig. 3B. Changes over the first 30 min show a decrease in characteristic absorptions of  $[\text{Co}(\text{bdt})_2]^-$  with isosbestic points at 760 nm, 510 nm, and 410 nm (*SI Appendix, Fig. S8* provides a better visualization of the early changes). Over a longer timescale (>15 h), further loss of  $[\text{Co}(\text{bdt})_2]^-$  absorptions occurs. The isosbestic points are consistent with the formation of a single  $[\text{Co}(\text{bdt})_x(\text{DHLA})]^{n-}$  species ( $x = 1$  or 2), after which complete substitution of  $\text{bdt}^{2-}$  by DHLA at the Co ion occurs. Whereas the spectroscopic experiment indicates slow ligand exchange at Co, the photochemical generation of  $\text{H}_2$  involves reduction of Co from formally 3+ to lower oxidation states that are more labile for ligand substitution. We conclude that DHLA substitutes for the bdt ligand at the Co ion, forming a complex that is greatly reduced in catalytic activity for  $\text{H}_2$  generation.

The second set of experiments was based on the inertness of the tripod capping agents **1** and **2** from the surface of CdSe NCs coupled with the excellent catalytic activity of  $[\text{Co}(\text{bdt})_2]^-$ . As shown in Fig. 4, systems composed of **1**- and **2**-CdSe NCs (5.0  $\mu\text{M}$ ),  $[\text{Co}(\text{bdt})_2]^-$  (0.8  $\mu\text{M}$ ), and AA (0.5 M) in  $\text{H}_2\text{O}$  (5.0 mL) at pH 4.5 upon irradiation with 520 nm light produced  $\text{H}_2$  with TONs over 300,000 (60 h) and TOFs of more than 5,500/h for 30 h. No loss of activity was observed over 30 h and only a slight decline thereafter as the concentration of AA decreased. After photolysis, the NCs were separated from the catalytic solutions by centrifugation. Upon addition of water to the centrifuged NCs and adjustment of the pH of the medium to slightly basic, a clear solution was obtained that showed an absorption spectrum similar to ones of the original NC solutions (*SI Appendix, Fig. S11*). Here it should be noted that the analogous DHLA-CdSe NCs after photolysis became insoluble, possibly due to dissociation of DHLA from the NCs' consequent aggregation (82). Measurements of

quantum yields for the two systems with **1** and **2** as capping agents based on power meter measurements to determine net photon flux and quantitative GC analysis of headspace gas at the conclusion of irradiation (*Materials and Methods*) gave values of  $24 \pm 4\%$  and  $25 \pm 3\%$  for **1**- and **2**-CdSe NC systems, respectively.

Further confirmation of the deleterious effect of DHLA on  $[\text{Co}(\text{bdt})_2]^-$  as a catalyst was provided by 520-nm irradiation of the **1**- and **2**-CdSe NC/ $[\text{Co}(\text{bdt})_2]^-$ /AA system to which DHLA (2 eq relative to catalyst) was added. The system proved to have significantly diminished activity (*SI Appendix, Fig. S12*), consistent with the notion of DHLA/bdt exchange at Co leading to formation of a substantially less active catalyst.

To address the question of whether the catalyst was free in solution or bound in some manner to the photosensitizer, the **1**-CdSe NC/ $[\text{Co}(\text{bdt})_2]^-$ /AA system was examined following  $\text{H}_2$  photogeneration. Specifically, after irradiation of the system, the NCs were separated from the aqueous solution by centrifugation. Neither the separated NCs nor the centrifuged solutions were found to have significant  $\text{H}_2$ -generating activity after adding aqueous ascorbic acid (0.5 M) to each. However, upon the addition of fresh  $[\text{Co}(\text{bdt})_2]^-$  to the centrifuged NCs or the addition of **1**-CdSe NCs to the centrifuged solution, both samples regained activity that was within 10% of the initial value (*SI Appendix, Fig. S13*). Any deviation in activity appears to be within the limits of instrumental and reconstitution errors, with  $\text{H}_2$  evolution plots showing constant activity. From these experiments, we conclude that the system is biphasic with the  $[\text{Co}(\text{bdt})_2]^-$  catalyst remaining in solution and the CdSe NCs maintaining their solid-phase integrity during the light-driven generation of  $\text{H}_2$ .

The absence of dissociation of **1** or **2** from CdSe NCs to which they are bound made possible an examination of different catalyst complexes. In this context, three other Co bis dithiolene complexes— $[\text{Co}(\text{tdt})_2]^-$ ,  $[\text{Co}(\text{Cl}_2\text{bdt})_2]^-$ , and  $[\text{Co}(\text{Cl}_4\text{bdt})_2]^-$ , where tdt is toluene-3,4-dithiolate,  $\text{Cl}_2\text{bdt}$  is 3,6-dichlorobenzene-1,2-dithiolate, and  $\text{Cl}_4\text{bdt}$  is 3,4,5,6-tetrachloro-1,2-benzenedithiolate (Scheme 2)—were examined relative to  $[\text{Co}(\text{bdt})_2]^-$  to determine their relative effectiveness in  $\text{H}_2$  generation. The results are shown in Fig. 5 under the same conditions and concentrations for all of the catalysts. The order of activity in terms of turnovers at the end of 46 h of irradiation is  $[\text{Co}(\text{tdt})_2]^- > [\text{Co}(\text{bdt})_2]^- > [\text{Co}(\text{Cl}_2\text{bdt})_2]^- > [\text{Co}(\text{Cl}_4\text{bdt})_2]^-$  with TONs of 55,238, 53,303, 26,815, and 14,375, respectively. This order is inverse to the ease of reduction of the

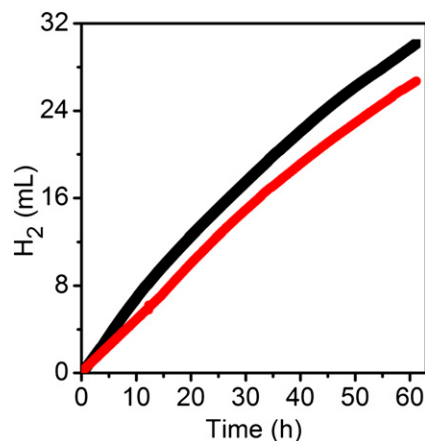


**Fig. 4.** Photocatalytic hydrogen production from a system containing **1**-CdSe NCs (530 nm) (5.0  $\mu\text{M}$ ) (red) or **2**-CdSe NCs (530 nm) (5.0  $\mu\text{M}$ ) (black),  $[\text{Co}(\text{bdt})_2]^-$  (0.8  $\mu\text{M}$ ), and AA (0.5 M) in  $\text{H}_2\text{O}$  (5.0 mL) at pH 4.5 upon irradiation with 520 nm LED at 15 °C and 1 atm initial pressure of  $\text{N}_2:\text{CH}_4$  (79:21 mol %) with  $\text{CH}_4$  as an internal standard for  $\text{H}_2$  quantification by GC analysis.

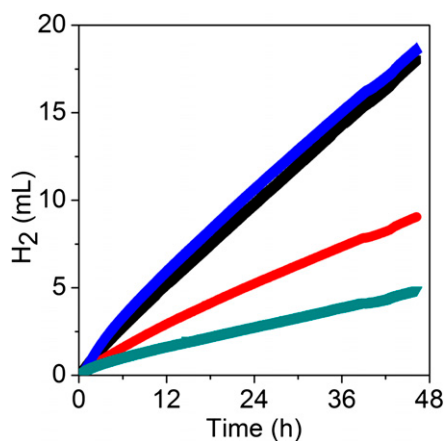


**Fig. 5.** Photocatalytic hydrogen production from a system containing 1-CdSe NCs (520 nm) (3  $\mu$ M) and AA (0.5 M) in H<sub>2</sub>O (5.0 mL) at pH 4.5 with different cobalt catalysts at 3  $\mu$ M {[Co(tdt)<sub>2</sub>]<sup>−</sup> (blue), [Co(bdt)<sub>2</sub>]<sup>−</sup> (black), [Co(Cl<sub>2</sub>bdt)<sub>2</sub>]<sup>−</sup> (red), and [Co(Cl<sub>4</sub>bdt)<sub>3</sub>]<sup>−</sup> (green)} upon irradiation with 520 nm LED at 15 °C and 1 atm initial pressure of N<sub>2</sub>:CH<sub>4</sub> (79:21 mol %) with CH<sub>4</sub> as an internal standard for H<sub>2</sub> quantification by GC analysis.

CoL<sub>2</sub><sup>−2−</sup> couple (−0.70, −0.64, −0.51, −0.40 V vs. SCE) (38). The two chlorinated complexes exist in the solid state as dimers with each Co ion having a 5-coordinate tetragonal pyramidal geometry (the Co-S<sub>apical</sub> bond is to the other CoL<sub>2</sub> moiety). Dimerization of this type has been seen previously for CoL<sub>2</sub><sup>−</sup> derivatives in which the dithiolene ligand appears to be less donating than bdt based on the CoL<sub>2</sub><sup>−2−</sup> couple (38, 89).

**Use of Ni(pyridylthiolate)<sub>3</sub><sup>−</sup> as a Catalyst.** Another complex that has been found to be active as a molecular catalyst for H<sub>2</sub> production is [Ni(pyS)<sub>3</sub>]<sup>−</sup> (pyS, pyridylthiolate; Scheme 2) in a system with FI as the light absorber and TEA as the sacrificial electron donor at pH 11 (37). In this system, the excited dye FI\* is quenched reductively by TEA, after which electron transfer occurs from the reduced dye to the Ni catalyst. Other derivatives have recently been reported for this catalyst that functions by dechelation and pyridine protonation (90). When [Ni(pyS)<sub>3</sub>]<sup>−</sup> was used as a catalyst with DHLA-CdSe NCs and ascorbic acid at pH 4.5, H<sub>2</sub>-generating activity was observed similar to that found when Ni(NO<sub>3</sub>)<sub>2</sub> was used as the catalyst, suggesting possible formation of the Ni DHLA catalyst by DHLA substitution of pyS<sup>−</sup>. This notion was supported by the observation that when [Ni(pyS)<sub>3</sub>]<sup>−</sup> was used with 1-CdSe NCs, the activity was greatly reduced, and when DHLA was added to the system, an increase in H<sub>2</sub>-generating activity was found (SI Appendix, Fig. S14). Again, the importance of ligand exchange from the NC surface to the potential catalyst is supported by this set of experiments.

**Electron Transfer from 1- and 2-CdSe NCs upon Irradiation.** A central question regarding the photosensitizer in any system for the light-driven reduction of protons is whether following its formation, PS\* transfers an electron to the catalyst (or an electron mediator) or accepts an electron from the sacrificial electron donor (or an electron mediator). The former is oxidative quenching of the excited state whereas the latter is reductive quenching. For the previously reported DHLA-CdSe NCs/Ni(NO<sub>3</sub>)<sub>2</sub>/AA system, it was determined that irradiation of DHLA-CdSe NCs in the presence of known electron acceptors led to spectroscopic observation of the reduced electron acceptors. For the light absorbers 1- and 2-CdSe NCs in the present study, it was found that both MV<sup>2+</sup> and DQ<sup>2+</sup> (where MV<sup>2+</sup> is dimethyl-4,4'-bipyridinium and DQ<sup>2+</sup> is N,N'-(1,3-propylene)-5,5'-dimethyl-2,2'-bipyridinium) are converted into their respective cation

radicals when a solution containing them and 1- or 2-CdSe NCs is irradiated with 520 nm light. The radical cations MV<sup>+</sup> and DQ<sup>+</sup>, which are blue and pink, respectively, were identified both visually and spectroscopically (SI Appendix, Fig. S16). The reduction potential for DQ<sup>2+</sup> [−0.7 V vs. normal hydrogen electrode (NHE)] is more negative than that for MV<sup>2+</sup> (−0.44 V vs. NHE) (91), indicating that the conduction band electron from CdSe NCs must be more negative than −0.7 V vs. NHE. These measurements are consistent with published cyclic voltammetric studies that indicate a reduction potential more negative than −1 V for CdSe NCs of this size (92).

**Formation of H<sub>2</sub>.** Based on the observations of electron transfer from the S<sub>3</sub>-capped CdSe NCs to dialkylated bipyridinium acceptors, it can be assumed that the initial step in H<sub>2</sub> generation is reduction of the catalyst [Co(bdt)<sub>2</sub>]<sup>−</sup> (or one of its derivatives) to the dianion [Co(bdt)<sub>2</sub>]<sup>2−</sup> that is formally Co(II). However, the frontier orbitals of [Co(bdt)<sub>2</sub>]<sup>−</sup> and similar Co bis dithiolene derivatives are known to have significant ligand character so that traditional oxidation state assignments are useful only for electron bookkeeping (93). Previously, Solis and Hammes-Schiffer performed a theoretical analysis of [Co(bdt)<sub>2</sub>]<sup>−</sup> and related dithiolenes in terms of the steps leading to H<sub>2</sub> generation (94). According to Solis and Hammes-Schiffer, following initial reduction, the Co bis dithiolene complex undergoes protonation at one of the S donors. Depending on the nature of the dithiolene, the resultant Co(H-dithiolene)(dithiolene)<sup>−</sup> species will undergo either a second protonation or a 1 e<sup>−</sup> reduction. If the former, this step is followed by a 1 e<sup>−</sup> reduction; if the latter, this step is followed by a second protonation. The question of whether to undergo a second protonation or a 1 e<sup>−</sup> reduction is based on the donicity of the dithiolene. With bdt<sup>2−</sup>, it appears that a second protonation is favored, whereas with a more electron-withdrawing ligand such as mnt<sup>2−</sup> (mnt, maleonitriledithiolate) the 1 e<sup>−</sup> reduction is preferred. In either case, the paths lead to an intermediate that is formally Co(I) with two protonated dithiolenes. All of the elements for H<sub>2</sub> have been assembled at the catalyst. A proton transfer within this intermediate yields a Co(III)-H(SH) species that is set for heterocoupling of H<sup>−</sup> and H<sup>+</sup> to give H<sub>2</sub> with regeneration of the Co(dithiolene)<sub>2</sub><sup>−</sup> monoanion.

Based on the order of activity that we find—i.e., [Co(tdt)<sub>2</sub>]<sup>−</sup> > [Co(bdt)<sub>2</sub>]<sup>−</sup> > [Co(Cl<sub>2</sub>bdt)<sub>2</sub>]<sup>−</sup> > [Co(Cl<sub>4</sub>bdt)<sub>3</sub>]<sup>−</sup>—and the fact that the conduction band electron from excited CdSe NCs is energetic enough to reduce all of the [Co(bdt)<sub>2</sub>]<sup>−</sup> derivatives and diprotonated derivatives, we speculate that the heterocoupling step may be the turnover-limiting step and that the more hydridic the Co hydride intermediate is, the faster the H<sup>−</sup>-H<sup>+</sup> coupling to yield H<sub>2</sub>. The observed order of activity would be consistent with this analysis with the most difficult to reduce complex, [Co(tdt)<sub>2</sub>]<sup>−</sup>, giving the most basic Co(I) and the most hydridic intermediate. Although a basis for understanding the current system has been developed, more work remains to be done in testing experimentally the proposed mechanism of formation.

Very recently, another system using water-solubilized CdSe QDs as the photosensitizer has been reported by Wu et al. (95). The water-solubilizing agent is 3-mercaptopropionic acid (MPA) whereas the catalyst is an Fe<sub>2</sub>S<sub>2</sub> hydrogenase mimic bound to polyacrylic acid and the electron donor is AA. The light used was 450 nm from a blue LED source with the QDs having an excitonic maximum at 470 nm. Although the relative activity and quantum yield for H<sub>2</sub> generation are lower than those reported here and previously, the results cannot be compared directly because of many differences in the conditions and analyses. It is evident that this system has significant amounts of free MPA in solution during photolysis, which can undergo ligand exchange with the catalyst. For comparison, an Fe catalyst different from the one used by Wu et al. was examined by us, using the system employed in the present study. Our results indicate that

$\text{Fe}(\text{bdt})_2^-$  as the catalyst exhibits only 25% of the activity of  $[\text{Co}(\text{bdt})_2]^-$  (SI Appendix, Fig. S17).

## Conclusions

The principal conclusion from the study described in this paper is that the dynamics of surface stabilizing and solubilizing agents are important in the analysis of any system in which semiconductor NCs are used as the light-absorbing photosensitizer. Through the use of capping agents **1** and **2** with a  $-\text{C}(\text{CH}_2\text{-S})_3$  motif, dissociation from the surface has been made negligible, thereby removing any exchange reactions between the solubilizing agent and ligands on the catalyst in solution. This type of exchange was found to influence negatively the behavior of Co bis dithiolene catalysts and affect positively the activity of potential Ni catalysts by formation of a Ni-DHLA complex in situ (82). The absence of capping agent dissociation from **1**- and **2**-CdSe made possible a meaningful examination of  $[\text{Co}(\text{bdt})_2]^-$  and several derivatives as  $\text{H}_2$ -generating catalysts. The activity of these catalysts was found to increase with increasing donicity. The activity and stability of systems having NCs capped with agents such as **1** and **2** as photosensitizers raise the possibility of these components functioning in an artificial photosynthetic water-splitting system.

## Materials and Methods

**Materials.** All starting materials were purchased from Aldrich unless otherwise mentioned. Pentaerythritoltribromide was purchased from AK Scientific and used without further purification. All solvents were dried before use. For photocatalytic experiments, deionized water was used. The syntheses of CdSe-TOPO NCs,  $(^i\text{Bu}_4\text{N})[\text{Co}(\text{bdt})_2]$  and  $(\text{Et}_4\text{N})[\text{Ni}(\text{pyS})_3]$  were done following literature procedures (37, 39, 88).

**Instrumentation.**  $^1\text{H}$  NMRs were recorded on a Bruker Avance 400-MHz spectrometer and referenced to either a residual proton resonance of the deuterated solvent or tetramethylsilane as an internal standard. UV-vis spectra were recorded on a Cary 60 UV-vis spectrophotometer, using a 1-cm path length quartz cuvette in acetonitrile. Elemental analyses were performed using a PerkinElmer 2400 Series II Analyzer.

**Preparation of 3-Bromo-2,2-bis(bromomethyl)propanoic Acid.** The synthesis of this compound followed the reported procedure with minor changes (96). A mixture of 12 mL of conc.  $\text{HNO}_3$  and fuming  $\text{HNO}_3$  (9:1) was heated to 70 °C. To this mixture, 3.0 g (0.009 mol) of pentaerythritoltribromide was added over 15 min. The mixture was then heated at 90 °C for 3 h, during which fumes of brown nitrogen dioxide evolved. The warm reaction mixture was poured into 150 mL iced water with vigorous stirring. A white powder precipitated from the solution and was collected by filtration, followed by washing three times with ice-cold water, and dried under vacuum. Yield was 2.80 g (90%). Elemental analyses Calcd. for  $\text{C}_5\text{H}_7\text{Br}_3\text{O}_2$ : C, 17.72; H, 2.08. Found: C, 17.70; H, 1.96.  $^1\text{H}$ -NMR in  $\text{CDCl}_3$  [ $\delta$ /ppm]: 11.97 (bs, 1H), 3.76 (s, 6H).  $^{13}\text{C}$ -NMR in  $\text{CDCl}_3$  [ $\delta$ /ppm]: 173.9, 53.2, 32.6.

**Synthesis of 3-Mercapto-2,2-bis(mercaptomethyl)propanoic Acid (1).** A total of 3.3 g (~35 mmol) of  $\text{NaSH}\cdot x\text{H}_2\text{O}$  was dissolved in 25 mL of distilled water and degassed by bubbling  $\text{N}_2$  through the solution. To this mixture, 2.0 g (5.96 mmol) of 3-bromo-2,2-bis(bromomethyl)propanoic acid was added over 30 min, after which the mixture was refluxed for 24 h and cooled. The reaction mixture was treated with conc.  $\text{H}_2\text{SO}_4$  at 15 °C until evolution of  $\text{H}_2\text{S}$  ceased and then was extracted with dichloromethane. The combined organic layer was dried over anhydrous  $\text{Na}_2\text{SO}_4$  and evaporated under reduced pressure. The solid obtained was dissolved in 30 mL 0.25 M  $\text{NaHCO}_3$  solution, treated with excess  $\text{NaBH}_4$  at 0 °C, and stirred for 3 h. The reaction mixture was treated with 6 N HCl until it was acidic (pH ~ 4) and extracted with dichloromethane (3  $\times$  25 mL). The combined organic layer was dried over anhydrous  $\text{Na}_2\text{SO}_4$ . Evaporation of the solvent under reduced pressure gave **1** as a pale yellow solid. Yield: 0.80 g (68%). Elemental analyses Calcd. for  $\text{C}_5\text{H}_{10}\text{O}_2\text{S}_3$ : 30.28; H, 5.08. Found: C, 30.52; H, 4.99.  $^1\text{H}$ -NMR in  $\text{CDCl}_3$  [ $\delta$ /ppm]: 11.58 (bs, 1H), 3.01 (d, 6H,  $J = 9.07$  Hz), 1.43 (t, 3H,  $J = 9.06$  Hz).  $^{13}\text{C}$ -NMR in  $\text{CDCl}_3$ : 179.1, 54.3, 27.6.

**Synthesis of 2-(3-Bromo-2,2-bis(bromomethyl)propoxy)acetic Acid.** Ten grams (31 mmol) of pentaerythritol tribromide and 6.5 g (31 mmol) of sodium iodoacetate were mixed together and degassed, followed by the addition of

50 mL of dry tetrahydrofuran. The mixture was kept at  $-78$  °C and 20 mL *n*-butyl lithium solution (1.6 M in hexane) was added dropwise over 1 h. After the addition, the reaction mixture was stirred at room temperature overnight. The reaction mixture was treated with 50 mL of water and 4 N hydrochloric acid to adjust the pH to ~4 and then extracted with ethyl acetate (3  $\times$  100 mL). The combined organic layers were evaporated under reduced pressure and purified by chromatography [silica gel (60 mesh), eluting solvents ethyl acetate/hexanes with the desired product obtained from a 5:95 solvent mixture]. Removal of the eluting solvent under reduced pressure gave 2-(3-bromo-2,2-bis(bromomethyl)propoxy)acetic acid as a white solid (7.1 g, ~60%). Elemental analyses Calcd. for  $\text{C}_7\text{H}_{11}\text{Br}_3\text{O}_3$ : C, 21.96; H, 2.90. Found: C, 22.04; H, 2.76.  $^1\text{H}$ -NMR in  $\text{CDCl}_3$  [ $\delta$ /ppm]: 10.68 (bs, 1H), 4.19 (s, 2H), 3.67 (s, 2H), 3.58 (s, 6H).  $^{13}\text{C}$ -NMR in  $\text{CDCl}_3$ : 175.9, 70.9, 68.3, 43.8, 34.7.

**Synthesis of 2-(3-Thiocyanato-2,2-bis(thiocyanatomethyl)propoxy)acetic Acid.** Two grams (5.2 mmol) of 2-(3-bromo-2,2-bis(bromomethyl)propoxy)acetic acid was added to a solution of potassium thiocyanate (3.0 g) in *N,N*-dimethylformamide (15 mL) at 100 °C under dinitrogen atmosphere. The temperature was then raised to 140 °C and maintained for 30 min. The reaction mixture was then cooled to room temperature and stirred overnight. The resulting suspension was diluted by adding 100 mL of water and extracted with ether (3  $\times$  50 mL). The combined ether layers were washed with brine (2  $\times$  50 mL) and dried over anhydrous  $\text{MgSO}_4$ . Evaporation of solvent under reduced pressure gave 2-(3-thiocyanato-2,2-bis(thiocyanatomethyl)propoxy)acetic acid as a pale yellow solid (1.41 g, 85%). Elemental analyses Calcd. for  $\text{C}_{10}\text{H}_{11}\text{N}_3\text{O}_3\text{S}_3$ : C, 37.84; H, 3.49; N, 13.24. Found: C, 37.51; H, 3.40, N, 12.86.  $^1\text{H}$ -NMR in  $\text{CDCl}_3$  [ $\delta$ /ppm]: 4.23 (s, 2H), 3.76 (s, 2H), 3.36 (s, 6H).  $^{13}\text{C}$ -NMR in  $\text{CDCl}_3$ : 173.1, 111.6, 70.3, 67.0, 46.4, 36.8.

**Synthesis of 2-(3-Mercapto-2,2-bis(mercaptomethyl)propoxy)acetic Acid (2).** To a solution of 2-(3-thiocyanato-2,2-bis(thiocyanatomethyl)propoxy)acetic acid (1.0 g, 3 mmol) in 25 mL absolute ethanol was added 1.5 g (39 mmol) of  $\text{NaBH}_4$  in small portions with stirring at room temperature. After stirring for 1 h at room temperature, the mixture was heated to reflux for 5–6 h. The reaction mixture was then cooled to room temperature and diluted with 100 mL of water. The pH of the resultant solution was adjusted to ~4 by addition of 1 M HCl and extracted with ether (100 mL). The ether layer was washed with water (50 mL) and dried over anhydrous  $\text{Na}_2\text{SO}_4$ . Upon removal of the solvent under reduced pressure, **2** was obtained as a pale yellow oil (0.65 g, 86%). Elemental analyses Calcd. for  $\text{C}_7\text{H}_{14}\text{O}_3\text{S}_3$ : C, 34.69; H, 5.82. Found: C, 35.30; H, 5.74.  $^1\text{H}$ -NMR in  $\text{CDCl}_3$  [ $\delta$ /ppm]: 9.86 (bs, 1H), 4.10 (s, 2H), 3.44 (s, 2H), 2.60 (d, 6H,  $J = 9.02$  Hz), 1.37 (t, 3H,  $J = 9.0$  Hz).  $^{13}\text{C}$ -NMR in  $\text{CDCl}_3$ : 175.9, 70.9, 68.3, 43.8, 34.7.

**Hydrogen Evolution Studies.** Samples were prepared in 40-mL scintillation vials and protected from light before use. Total volume of the solution in each sample was 5 mL, the pH adjusted by the addition of HCl or NaOH. The samples were placed into a temperature-controlled block at 15 °C and sealed with an air-tight cap fitted with a pressure transducer and a rubber septum. The samples were then purged with a mixture of gas containing 4:1  $\text{N}_2/\text{CH}_4$ . The methane present in the gas mixture serves as an internal reference for GC analysis at the end of the experiment. The samples were irradiated from below the vials with high-power Philips LumiLED Luxeon Star Hex green (520 nm) 700-mA LEDs. The light power of each LED was set to 70 mW and measured with an L30 A Thermal sensor and a Nova II power meter (Ophir-Spiricon). The samples were swirled using an orbital shaker. The pressure changes in the vials were recorded using a Labview program from a Free-scale semiconductor sensor (MPX4259A series). At the end of the experiment, the headspace of the vials was characterized by gas chromatography to ensure that the measured pressure change was a consequence of hydrogen generation and to confirm that the amount of hydrogen calculated by the change in pressure corresponded to the amount determined by GC. The amounts of hydrogen evolved were determined using a Shimadzu GC-17A gas chromatograph with a 5-Å molecular sieve column (30 m, 0.53 mm) and a thermal conductivity detector and were quantified by a calibration plot to the internal  $\text{CH}_4$  standard.

**Synthesis of 1- or 2-Capped CdSe NCs.** A total of 570  $\mu\text{L}$  of 25% tetraethyl ammonium hydroxide was added to 10 mL of methanol containing 200 nmol of CdSe-TOPO. The mixture was degassed by bubbling  $\text{N}_2$  through the solution and kept under a stream of  $\text{N}_2$ . Eighty milligrams of **1** (or for 2-CdSe, 100 mg of **2**) was dissolved in 2 mL of dry methanol, degassed, and added by cannula to the previously degassed mixture of CdSe-TOPO and base. The mixture was then heated at 65 °C for 6 h under inert atmosphere. The **1**- or



2-capped CdSe NCs were precipitated from the methanolic solution by the addition of ethyl acetate and separated by centrifugation ( $3,399 \times g$ ). The procedure was repeated twice more to ensure the removal of all unreacted ligand. The washed 1-CdSe or 2-CdSe NCs were suspended in slightly basic water (pH  $\sim 8.0$ ) and stored in a freezer.

**Characterization of the Quantum Dots.** UV-vis absorption spectra were recorded on a Cary 60 UV/vis spectrophotometer. Aqueous quantum dot samples were dissolved in water solution and placed in a 1-cm path length cuvette. UV-vis spectra of the TOPO-capped NCs were measured by using hexane as the solvent; whereas those of 1-CdSe or 2-CdSe were measured in water.

**NMR Experiment on Tripod Capped CdSe.** The pH of a 15.6- $\mu\text{M}$  solution of 1-CdSe or 2-CdSe was adjusted to 4.5 by addition of HCl. The mixture was degassed well and stirred for 24 h. The NCs were removed by centrifugation (4,000 rpm) and solvent was evaporated. The residue was dissolved in 1 mL acetonitrile- $d_3$  containing  $5.0 \times 10^{-7}$  mol of benzene as an internal standard. The  $^1\text{H}$  NMR spectrum was recorded on a Bruker Avance 400-MHz spectrometer, but resonances due to the capping ligand were not observed.

**Quantum Yield Measurement.** The difference between the light passing through the blank solution (containing 0.5 M AA at pH 4.5) and the sample containing 0.5 M AA and the CdSe NCs with varying concentrations at pH 4.5 was used to calculate the light absorbed by the NCs in each sample. The difference in power of the light  $P$  (in watts) was measured by using an L30

A Thermal Sensor and a Nova II power meter (Ophir-Spiricon). The average rate of the hydrogen production  $k$  (mol  $\text{H}_2/\text{s}$ ) was calculated from the amount of hydrogen generated from the first 10 h of light irradiation. The quantum yield  $\phi$  for  $\text{H}_2$  generation was calculated using the equation

$$P = \frac{c \times h \times n}{\lambda \times t}; \quad q_p = n/t$$

$$q_p = \frac{(P \times \lambda)}{(c \times h)}$$

$$\text{Quantum Yield } (\phi) = \frac{2 \times \text{average rate of hydrogen production } (k)}{\text{photon flux } (q_p)} \times 100 \%$$

where  $\lambda$  is taken as 520 nm for the green LED light source,  $h$  is Planck's constant (Joules per second),  $c$  is the velocity of light (meters per second),  $n$  is the number of photons absorbed,  $t$  is the time (seconds), and  $q_p$  is the photon flux (number of photons per second) absorbed by the NCs. The average of the quantum yields for identical samples was calculated with uncertainties based on the multiple measurements.

**ACKNOWLEDGMENTS.** We thank William Eckenhoff and Randy Sabatini for helpful discussions. This work is supported by the Division of Chemical Sciences, Geosciences, and Biosciences, Office of Basic Energy Sciences, US Department of Energy, Grant DE-FG02-09ER16121.

- Esswein AJ, Nocera DG (2007) Hydrogen production by molecular photocatalysis. *Chem Rev* 107(10):4022–4047.
- Nocera DG (2009) Chemistry of personalized solar energy. *Inorg Chem* 48(21):10001–10017.
- Eisenberg R (2009) Chemistry. Rethinking water splitting. *Science* 324(5923):44–45.
- Gray HB (2009) Powering the planet with solar fuel. *Nat Chem* 1(1):7.
- Blankenship RE (2002) *Molecular Mechanisms of Photosynthesis* (Blackwell, Oxford).
- Lawlor DW (2001) *Photosynthesis* (Springer, New York).
- Gregory RPF (1977) *Biochemistry of Photosynthesis* (Wiley Interscience, New York).
- Youngblood WJ, et al. (2009) Photoassisted overall water splitting in a visible light-absorbing dye-sensitized photoelectrochemical cell. *J Am Chem Soc* 131(3):926–927.
- Alstrum-Acevedo JH, Brennaman MK, Meyer TJ (2005) Chemical approaches to artificial photosynthesis. 2. *Inorg Chem* 44(20):6802–6827.
- Meyer TJ (1989) Chemical approaches to artificial photosynthesis. *Acc Chem Res* 22(5):163–170.
- Grätzel M (1981) Artificial photosynthesis: Water cleavage into hydrogen and oxygen by visible light. *Acc Chem Res* 14(12):376–384.
- Eisenberg R, Nocera DG (2005) Preface: Overview of the forum on solar and renewable energy. *Inorg Chem* 44(20):6799–6801.
- Chakraborty S, Wadas TJ, Hester H, Schmehl R, Eisenberg R (2005) Platinum chromophore-based systems for photoinduced charge separation: A molecular design approach for artificial photosynthesis. *Inorg Chem* 44(20):6865–6878.
- Hara M, et al. (1998)  $\text{Cu}_2\text{O}$  as a photocatalyst for overall water splitting under visible light irradiation. *Chem Commun* (3):357–358.
- Khaselev O, Turner JA (1998) A monolithic photovoltaic-photoelectrochemical device for hydrogen production via water splitting. *Science* 280(5362):425–427.
- Tsuji I, Kato H, Kobayashi H, Kudo A (2004) Photocatalytic  $\text{H}_2$  evolution reaction from aqueous solutions over band structure-controlled  $(\text{AgIn})_x\text{Zn}_{2(1-x)}\text{S}_2$  solid solution photocatalysts with visible-light response and their surface nanostructures. *J Am Chem Soc* 126(41):13406–13413.
- Lehn JM, Sauvage JP (1977) Chemical storage of light energy. Catalytic generation of hydrogen by visible light or sunlight. Irradiation of neutral aqueous solutions. *Nouv J Chim* 1(6):449–451.
- Krishnan CV, Sutin N (1981) Homogeneous catalysis of the photoreduction of water by visible light. 2. Mediation by a tris(2,2'-bipyridine)ruthenium(II)-cobalt(II) bipyridine system. *J Am Chem Soc* 103(8):2141–2142.
- Keller P, Moradpour A, Amouyal E, Kagan HB (1980) Hydrogen production by visible-light using viologen-dye mediated redox cycles. *Nouv J Chim* 4(6):377–384.
- Kirch M, Lehn J-M, Sauvage J-P (1979) Hydrogen generation by visible light irradiation of aqueous solutions of metal complexes. An approach to the photochemical conversion and storage of solar energy. *Helv Chim Acta* 62(4):1345–1384.
- Moradpour A, Amouyal E, Keller P, Kagan H (1978) Hydrogen production by visible light irradiation of aqueous solutions of tris(2,2'-bipyridine)ruthenium(2+). *Nouv J Chim* 2(6):547–549.
- Kalyanasundaram K, Kiwi J, Grätzel M (1978) Hydrogen evolution from water by visible light, a homogeneous three component test system for redox catalysis. *Helv Chim Acta* 61(7):2720–2730.
- Launikonis A, et al. (1982) Solar reduction of water. III. Improved electron-transfer agents for the system water-Tris(2,2'-bipyridine)ruthenium dication-ethylenediaminetetraacetic acid-platinum. *Aust J Chem* 35(7):1341–1355.
- Johansen O, et al. (1981) Solar reduction of water. I. Competition between light-induced hydrogen formation and hydrogenation of methylviologen in the system water-Tris(2,2'-bipyridine)ruthenium dication-ethylenediaminetetraacetic acid-platinum. *Aust J Chem* 34(5):981–991.
- Furlong DN, Wells D, Sasse WHF (1986) Colloidal semiconductors in systems for the sacrificial photolysis of water: Sensitization of titanium dioxide by adsorption of ruthenium complexes. *J Phys Chem* 90(6):1107–1115.
- Palmans R, Frank AJ (1991) A molecular water-reduction catalyst: Surface derivatization of titania colloids and suspensions with a platinum complex. *J Phys Chem* 95(23):9438–9443.
- Borgarello E, Kiwi J, Pelizzetti E, Visca M, Grätzel M (1981) Photochemical cleavage of water by photocatalysis. *Nature* 289(5794):158–160.
- Furlong DN, Wells D, Sasse WHF (1985) Colloidal semiconductors in systems for the sacrificial photolysis of water. 2. Hydrogen production with platinum/titanium dioxide catalysts. *J Phys Chem* 89(10):1922–1928.
- Hawecker J, Lehn JM, Ziesel R (1983) Efficient homogeneous photochemical hydrogen generation and water reduction mediated by cobaloxime or macrocyclic cobalt complexes. *Nouv J Chim* 7(5):271–277.
- McLaughlin MP, McCormick TM, Eisenberg R, Holland PL (2011) A stable molecular nickel catalyst for the homogeneous photogeneration of hydrogen in aqueous solution. *Chem Commun* 47(28):7989–7991.
- Streich D, et al. (2010) High-turnover photochemical hydrogen production catalyzed by a model complex of the [FeFe]-hydrogenase active site. *Chemistry* 16(1):60–63.
- Jasimuddin S, Yamada T, Fukuju K, Otsuki J, Sakai K (2010) Photocatalytic hydrogen production from water in self-assembled supramolecular iridium-cobalt systems. *Chem Commun* 46(44):8466–8468.
- Goldsmith JI, Hudson WR, Lowry MS, Anderson TH, Bernhard S (2005) Discovery and high-throughput screening of heteroleptic iridium complexes for photoinduced hydrogen production. *J Am Chem Soc* 127(20):7502–7510.
- Lowry MS, et al. (2005) Single-layer electroluminescent devices and photoinduced hydrogen production from an ionic iridium(III) complex. *Chem Mater* 17(23):5712–5719.
- Na Y, et al. (2008) Visible light-driven electron transfer and hydrogen generation catalyzed by bioinspired [2Fe2S] complexes. *Inorg Chem* 47(7):2805–2810.
- Luo S-P, et al. (2013) Photocatalytic water reduction with copper-based photosensitizers: A noble-metal-free system. *Angew Chem Int Ed Engl* 52(1):419–423.
- Han Z, McNamara WR, Eum M-S, Holland PL, Eisenberg R (2012) A nickel thiolate catalyst for the long-lived photocatalytic production of hydrogen in a noble-metal-free system. *Angew Chem Int Ed Engl* 51(7):1667–1670.
- McNamara WR, et al. (2012) Cobalt-dithiolene complexes for the photocatalytic and electrocatalytic reduction of protons in aqueous solutions. *Proc Natl Acad Sci USA* 109(39):15594–15599.
- McNamara WR, et al. (2011) A cobalt-dithiolene complex for the photocatalytic and electrocatalytic reduction of protons. *J Am Chem Soc* 133(39):15368–15371.
- Tinker LL, et al. (2007) Visible light induced catalytic water reduction without an electron relay. *Chemistry* 13(31):8726–8732.
- Gärtner F, et al. (2009) Light-driven hydrogen generation: Efficient iron-based water reduction catalysts. *Angew Chem Int Ed Engl* 48(52):9962–9965.
- Helm ML, Stewart MP, Bullock RM, DuBois MR, DuBois DL (2011) A synthetic nickel electrocatalyst with a turnover frequency above 100,000  $\text{s}^{-1}$  for  $\text{H}_2$  production. *Science* 333(6044):863–866.
- Lawrence JD, Li H, Rauchfuss TB, Bénard M, Rohmer M-M (2012) Diiron azadithiolates as models for the iron-only hydrogenase active site: Synthesis, structure, and stereo-electronics. This research was supported by the NIH and the Centre Universitaire et Régional de Ressources Informatiques of ULP and CNRS. *Angew Chem Int Ed Engl* 40(9):1768–1771.
- Connolly P, Espenson JH (1986) Cobalt-catalyzed evolution of molecular hydrogen. *Inorg Chem* 25(16):2684–2688.

45. Baffert C, Artero V, Fontecave M (2007) Cobaloximes as functional models for hydrogenases. 2. Proton electroreduction catalyzed by difluoroboryl-bis(dimethylglyoximate)cobalt(II) complexes in organic media. *Inorg Chem* 46(5):1817–1824.
46. Razavet M, Artero V, Fontecave M (2005) Proton electroreduction catalyzed by cobaloximes: Functional models for hydrogenases. *Inorg Chem* 44(13):4786–4795.
47. Jacques P-A, Artero V, Pécaut J, Fontecave M (2009) Cobalt and nickel diimine-dioxime complexes as molecular electrocatalysts for hydrogen evolution with low overpotentials. *Proc Natl Acad Sci USA* 106(49):20627–20632.
48. Hu X, Brunschwig BS, Peters JC (2007) Electrocatalytic hydrogen evolution at low overpotentials by cobalt macrocyclic glyoxime and tetraimine complexes. *J Am Chem Soc* 129(29):8988–8998.
49. Stubbert BD, Peters JC, Gray HB (2011) Rapid water reduction to H<sub>2</sub> catalyzed by a cobalt bis(iminopyridine) complex. *J Am Chem Soc* 133(45):18070–18073.
50. McCrory CCL, Uyeda C, Peters JC (2012) Electrocatalytic hydrogen evolution in acidic water with molecular cobalt tetraazamacrocycles. *J Am Chem Soc* 134(6):3164–3170.
51. Fihri A, et al. (2008) Cobaloxime-based photocatalytic devices for hydrogen production. *Angew Chem Int Ed Engl* 47(3):564–567.
52. Fihri A, Artero V, Pereira A, Fontecave M (2008) Efficient H<sub>2</sub>-producing photocatalytic systems based on cyclometalated iridium- and tricarboxylrhodium-diimine photosensitizers and cobaloxime catalysts. *Dalton Trans* 0(41):5567–5569.
53. Du P, Knowles K, Eisenberg R (2008) A homogeneous system for the photogeneration of hydrogen from water based on a platinum(II) terpyridyl acetylde chromophore and a molecular cobalt catalyst. *J Am Chem Soc* 130(38):12576–12577.
54. Du P, Schneider J, Luo G, Brennessel WW, Eisenberg R (2009) Visible light-driven hydrogen production from aqueous protons catalyzed by molecular cobaloxime catalysts. *Inorg Chem* 48(11):4952–4962.
55. Lazarides T, et al. (2009) Making hydrogen from water using a homogeneous system without noble metals. *J Am Chem Soc* 131(26):9192–9194.
56. McCormick TM, et al. (2011) Impact of ligand exchange in hydrogen production from cobaloxime-containing photocatalytic systems. *Inorg Chem* 50(21):10660–10666.
57. McCormick TM, et al. (2010) Reductive side of water splitting in artificial photosynthesis: New homogeneous photosystems of great activity and mechanistic insight. *J Am Chem Soc* 132(44):15480–15483.
58. Eckenhoff WT, Eisenberg R (2012) Molecular systems for light driven hydrogen production. *Dalton Trans* 41(42):13004–13021.
59. Du P, Eisenberg R (2012) Catalysts made of earth-abundant elements (Co, Ni, Fe) for water splitting: Recent progress and future challenges. *Energy Environ Sci* 5(3):6012–6021.
60. Eckenhoff WT, McNamara WR, Du P, Eisenberg R (2013) Cobalt complexes as artificial hydrogenases for the reductive side of water splitting. *Biochim Biophys Acta* 1827(8–9):958–973.
61. Nocera DG (2009) Living healthy on a dying planet. *Chem Soc Rev* 38(1):13–15.
62. Losse S, Vos JG, Rau S (2010) Catalytic hydrogen production at cobalt centres. *Coord Chem Rev* 254(21–22):2492–2504.
63. Artero V, Chavarot-Kerlidou M, Fontecave M (2011) Splitting water with cobalt. *Angew Chem Int Ed Engl* 50(32):7238–7266.
64. King PW (2013) Designing interfaces of hydrogenase–nanomaterial hybrids for efficient solar conversion. *Biochim Biophys Acta* 1827(8–9):949–957.
65. Bard AJ, Fox MA (1995) Artificial photosynthesis: Solar splitting of water to hydrogen and oxygen. *Acc Chem Res* 28(3):141–145.
66. Fujishima A, Honda K (1972) Electrochemical photolysis of water at a semiconductor electrode. *Nature* 238(5358):37–38.
67. Chen X, Shen S, Guo L, Mao SS (2010) Semiconductor-based photocatalytic hydrogen generation. *Chem Rev* 110(11):6503–6570.
68. Kamat PV, Tvrdy K, Baker DR, Radich JG (2010) Beyond photovoltaics: Semiconductor nanoarchitectures for liquid-junction solar cells. *Chem Rev* 110(11):6664–6688.
69. Tada H, Fujishima M, Kobayashi H (2011) Photodeposition of metal sulfide quantum dots on titanium(IV) dioxide and the applications to solar energy conversion. *Chem Soc Rev* 40(7):4232–4243.
70. Chen X, Li C, Grätzel M, Kostecki R, Mao SS (2012) Nanomaterials for renewable energy production and storage. *Chem Soc Rev* 41(23):7909–7937.
71. Xiang Q, Yu J, Jaroniec M (2012) Graphene-based semiconductor photocatalysts. *Chem Soc Rev* 41(2):782–796.
72. Cowan AJ, Durrant JR (2013) Long-lived charge separated states in nanostructured semiconductor photoelectrodes for the production of solar fuels. *Chem Soc Rev* 42(6):2281–2293.
73. Osterloh FE (2013) Inorganic nanostructures for photoelectrochemical and photocatalytic water splitting. *Chem Soc Rev* 42(6):2294–2320.
74. Swierk JR, Mallouk TE (2013) Design and development of photoanodes for water-splitting dye-sensitized photoelectrochemical cells. *Chem Soc Rev* 42(6):2357–2387.
75. Yan H, et al. (2009) Visible-light-driven hydrogen production with extremely high quantum efficiency on Pt–PdS/CdS photocatalyst. *J Catal* 266(2):165–168.
76. Talapin DV, Lee J-S, Kovalenko MV, Shevchenko EV (2010) Prospects of colloidal nanocrystals for electronic and optoelectronic applications. *Chem Rev* 110(1):389–458.
77. Zhu H, Song N, Lv H, Hill CL, Lian T (2012) Near unity quantum yield of light-driven redox mediator reduction and efficient H<sub>2</sub> generation using colloidal nanorod heterostructures. *J Am Chem Soc* 134(28):11701–11708.
78. Wang F, et al. (2011) A highly efficient photocatalytic system for hydrogen production by a robust hydrogenase mimic in an aqueous solution. *Angew Chem Int Ed Engl* 50(14):3193–3197.
79. Brown KA, Wilker MB, Boehm M, Dukovic G, King PW (2012) Characterization of photochemical processes for H<sub>2</sub> production by CdS nanorod-[FeFe] hydrogenase complexes. *J Am Chem Soc* 134(12):5627–5636.
80. Shemesh Y, Macdonald JE, Menagen G, Banin U (2011) Synthesis and photocatalytic properties of a family of CdS-PdX hybrid nanoparticles. *Angew Chem Int Ed Engl* 50(5):1185–1189.
81. Holmes MA, Townsend TK, Osterloh FE (2012) Quantum confinement controlled photocatalytic water splitting by suspended CdSe nanocrystals. *Chem Commun* 48(3):371–373.
82. Han Z, Qiu F, Eisenberg R, Holland PL, Krauss TD (2012) Robust photogeneration of H<sub>2</sub> in water using semiconductor nanocrystals and a nickel catalyst. *Science* 338(6112):1321–1324.
83. Aldana J, Wang YA, Peng X (2001) Photochemical instability of CdSe nanocrystals coated by hydrophilic thiols. *J Am Chem Soc* 123(36):8844–8850.
84. Kloepper JA, Bradforth SE, Nadeau JL (2005) Photophysical properties of biologically compatible CdSe quantum dot structures. *J Phys Chem B* 109(20):9996–10003.
85. Clapp AR, Goldman ER, Mattoussi H (2006) Capping of CdSe-ZnS quantum dots with DHLA and subsequent conjugation with proteins. *Nat Protoc* 1(3):1258–1266.
86. Gravel E, et al. (2013) Compact tridentate ligands for enhanced aqueous stability of quantum dots and in vivo imaging. *Chem Sci* 4(1):411–417.
87. Camerano JA, Casado MA, Ciriano MA, Lahoz FJ, Oro LA (2005) A trithiol protio-ligand and its fixation to the periphery of a carbosilane dendrimer as scaffolds for polynuclear rhodium and iridium complexes and metallodendrimers. *Organometallics* 24(21):5147–5156.
88. Wang X, et al. (2009) Non-blinking semiconductor nanocrystals. *Nature* 459(7247):686–689.
89. Baker-Hawkes MJ, Dori Z, Eisenberg R, Gray HB (1968) The crystal and molecular structure of the tetra-n-butylammonium salt of the dianionic dimer of bis(1,2,3,4-tetrachlorobenzene-5,6-dithiolato)cobaltate. *J Am Chem Soc* 90(16):4253–4259.
90. Han Z, Shen L, Brennessel WW, Holland PL, Eisenberg R (2013) Series of nickel thiolate complexes for photocatalytic production of hydrogen from aqueous solutions in noble-metal-free systems. *J Am Chem Soc*, <http://dx.doi.org/10.1021/ja405257s>.
91. Ebbesen TW, Levey G, Patterson LK (1982) Photoreduction of methyl viologen in aqueous neutral solution without additives. *Nature* 298(5874):545–548.
92. Jasieniak J, Califano M, Watkins SE (2011) Size-dependent valence and conduction band-edge energies of semiconductor nanocrystals. *ACS Nano* 5(7):5888–5902.
93. Benedito FL, Petrenko T, Bill E, Weyhermüller T, Wiegardt K (2009) Square planar bis(3,6-bis(trimethylsilyl)benzene-1,2-dithiolato)metal complexes of Cr(II), Co(III), and Rh(II): An experimental and density functional theoretical study. *Inorg Chem* 48(23):10913–10925.
94. Solis BH, Hammes-Schiffer S (2012) Computational study of anomalous reduction potentials for hydrogen evolution catalyzed by cobalt dithiolene complexes. *J Am Chem Soc* 134(37):15253–15256.
95. Wang F, et al. (2013) Exceptional poly(acrylic acid)-based artificial [FeFe]-hydrogenases for photocatalytic H<sub>2</sub> production in water. *Angew Chem Int Ed* 52(31):8134–8138.
96. Axenrod T, Das KK, Yazdekhasti H, Dave PR, Stern AG (1997) An efficient synthesis of 3-bromo-2-(bromomethyl)-1-propene. *Org Prep Proced Int* 29(3):358–360.